Applied Mathematics & Information Sciences
An International Journal

http://dx.doi.org/10.18576/amis/200207

Impact of Multiplicative Noise on Kink Solitons in a Stochastic Higher-Order (2+1)-Dimensional Burgers System

Faisal Muteb K. Almalki

Department of Mathematics, Faculty of Science, Al-Baha University, Alaqiq, 65779-7738, Saudi Arabia

Received: 2 Dec. 2025, Revised: 22 Jan. 2026, Accepted: 26 Feb. 2026
Published online: 1 Mar. 2026

Abstract: This study investigates the stochastic higher-order (2+1)-dimensional Burgers equation, a nonlinear partial differential equation that incorporates both higher-order spatial derivatives and multiplicative noise to model complex wave phenomena in dissipative and randomly perturbed environments. Using the singular manifold method and a generalized Cole-Hopf transformation, explicit multi-kink soliton solutions are derived, capturing shock-like profiles and steep-gradient interactions. High-precision numerical simulations validate the analytical solutions and quantify the effects of noise intensity, wave number, and propagation speed. Results show that weak noise largely preserves soliton coherence, whereas stronger stochastic forcing produces pronounced deformations and may trigger instability. Overall, the study elucidates the coupled roles of nonlinearity, dispersion, and randomness, and advances the analysis of stochastic partial differential equations with relevance to fluid dynamics, spintronics, nonlinear optics, and stochastic signal processing.

Keywords: Soliton dynamics, Multiplicative white noise, WG system, chaotic processes, Wave transformation, Fluid dynamics, Burgers equation

1 Introduction

Nonlinear evolution equations of Korteweg–de Vries (KdV) and Burgers type constitute a central mathematical language for describing the emergence, interaction, and stability of coherent structures in dispersive–dissipative media, particularly in plasma environments. In higher-dimensional plasma models, the KdV-Zakharov-Kuznetsov (KdV-ZK) family has been derived to capture electron-acoustic and related wave modes, providing physically grounded reduced equations whose solutions encode solitary waves and other nonlinear patterns [1]. Motivated by these plasma applications, a large body of work has focused on obtaining exact traveling-wave and soliton solutions for modified KdV-ZK and viscous Burgers equations, employing constructive ansätze and systematic expansion techniques, including improved (G'/G)-expansion and exp-function methods, to generate broad classes of localized and periodic waveforms [2,3,14]. In parallel, the study of nonlinear structures in non-Maxwellian plasmas has highlighted rich phenomena such as soliton collisions and rogue-wave events within KdV/mKdV settings, emphasizing the sensitivity of coherent excitations to the underlying distributional physics and parameter regimes [5]. On the integrability and structural side, recursion-operator computation and symmetry-based frameworks remain fundamental tools for identifying conserved quantities, generating hierarchies, and organizing solution spaces for nonlinear PDEs, thereby linking exact solution theory with deeper algebraic and geometric mechanisms [6,7]. These methodologies have also supported the construction of periodic and special-function-based wave patterns in (2+1)-dimensional dispersive systems, extending the catalog of analytically tractable nonlinear dynamics beyond classical one-dimensional settings [8], while recent investigations continue to reveal complex waveforms (such as breather, rogue, rational, and periodic-kink structures) in vibration and continuum models governed by nonlinear evolution equations [9,10].

Within this broad landscape, Burgers-type models play a distinguished role as canonical representatives of

* Corresponding author e-mail: fmalmalki@bu.edu.sa

nonlinear convection combined with dissipation, and their higher-dimensional and higher-order generalizations provide an increasingly precise platform for capturing multi-directional transport and dispersive corrections. Classical studies have established multiple-front and coupled-front structures for Burgers systems, illustrating the rich interaction mechanisms available even in dissipative settings [11,12,13]. Subsequent developments have addressed (2+1)-dimensional and higher-order Burgers equations, yielding new exact solutions and analytical insights via integrability-oriented adaptations and singular manifold formulations [14,15]. Contemporary contributions have further expanded Burgers-like modeling to fractional space-time contexts, including geometrical investigations and solution construction for fractional-order families that more faithfully represent anomalous transport and memory effects [10]. In a complementary functional-analytic direction, advances on fractional and conformable derivative bases in Fréchet spaces have strengthened the approximation and convergence theory underpinning fractional operators and series representations that arise naturally in modern fractional PDE modeling [12,13].

These theoretical and methodological advances align closely with current interest in plasma-wave modeling via fractional KdV/mKdV frameworks: ion-acoustic shocks in warm-ion, isothermal-electron plasmas have been formulated through nonlinear space-time fractional KdV models [16,17], and conformable fractional mKdV settings have been shown to admit solitons, periodic solutions, and Hirota-bilinear multiwave constructions [18]. Moreover, the Hirota direct method and geometrical representations continue to generate multi-soliton solutions for coupled fractional nonlinear systems, underscoring the vitality of bilinearization and geometric viewpoints in fractional and multi-component settings [16]. Collectively, these strands motivate the present focus on higher-order and stochastic extensions of Burgers/KdV-type equations: such extensions aim to unify robust analytical solution construction with physically realistic modeling ingredients (e.g., multidimensionality, fractional operators, and noise), thereby enabling deeper understanding of stability, interaction, and long-time behavior of nonlinear wave structures across complex media [10,11,12,13,14,15,16,17,18].

Stochastic modeling has become indispensable for describing complex physical systems in which uncertainty, unresolved micro-scale variability, or environmental forcing produces observable macroscopic effects [19,20,21,22]. In many applications, randomness is most naturally represented through stochastic differential equations (SDEs) and stochastic partial differential equations (SPDEs), where a deterministic drift is augmented by a noise term (often idealized as a Wiener process) leading to mathematically well-posed models capable of capturing intermittency, fluctuations, and probabilistic long-time behavior. The foundational calculus and solution theory for such models are classically developed within the Itô framework, for which rigorous analytical and numerical treatments are presented in standard references on SDEs and SPDEs [23, 24,25]. Beyond classical smooth settings, modern probability theory has also advanced the analysis of multidimensional SDEs with irregular or distributional drift, including constructions that address singularities arising from white-noise potentials and related limiting objects; such developments provide a deeper structural basis for stochastic modeling in high-dimensional or highly rough regimes [26,27,28]. In parallel, stochastic ideas have been adopted in reduced-form modeling across the applied sciences, including conceptual climate models that encode the effects of unresolved variability through stochastic forcing mechanisms, thereby motivating analogous constructions in other nonlinear media [22].

In nonlinear wave theory, the role of noise is particularly pronounced because coherent structures such as solitons, breathers, and wave packets may undergo phase diffusion, amplitude jitter, or even qualitative transitions when subjected to random perturbations. Recent studies have investigated multiplicative-noise effects in optical and dispersive systems, for example by analyzing concatenation models in optical fibers under multiplicative stochasticity and deriving solution behavior under random modulation [19]. Related work has examined how multiplicative white noise modifies soliton propagation and stability in integrable or near-integrable evolution equations, including stochastic versions of the Gerdjikov–Ivanov equation and perturbed Triki–Biswas models, where noise can deform solitary profiles and alter interaction dynamics [20,21]. A closely aligned direction has focused on plasma-motivated nonlinear equations, where stochastic perturbations are introduced to quantify uncertainty in wave evolution; for instance, solitary-wave behavior under stochastic noise has been explored for the generalized Schamel equation [28]. More directly connected to KdV/mKdV-type dynamics, multiplicative white noise has been shown to significantly influence dynamical soliton solutions in the KdV equation, and corresponding analytical descriptions of stochastic soliton evolution have been developed to characterize the deformation of coherent structures under random forcing [29,30,31]. Furthermore, the combined presence of dissipation and stochasticity has been treated in damped mKdV settings, where analytical solutions are complemented by numerical simulations to illustrate how noise and damping jointly impact solitary-wave persistence and waveform morphology [32].

Alongside stochastic wave modeling, the control and manipulation of nonlinear and chaotic dynamics remains an important complementary theme, particularly when noise interacts with intrinsic instability and sensitive dependence on initial data. In this regard, linear control and anti-control strategies for chaotic systems offer conceptual tools for regulating complex trajectories, which is relevant when stochastic forcing is used either to

suppress undesirable chaotic behavior or to induce targeted transitions between dynamical regimes [29]. Collectively, the above works motivate the thesis-level viewpoint that multiplicative stochastic perturbations are not merely secondary corrections, but rather structurally significant mechanisms that can reshape coherent wave dynamics, modify stability landscapes, and influence long-time statistical behavior. Consequently, the synthesis of rigorous SDE/SPDE theory [23,24,25,26,27] with contemporary stochastic soliton investigations [19,20,21, 28,30,31,32] provides a coherent methodological foundation for analyzing noise-driven nonlinear wave propagation and for developing control-informed interpretations of stochastic, potentially chaotic, evolution in complex physical media [22,29]. This study focuses on the investigation of N-kink soliton solutions and their stability under multiplicative noise in the stochastic higher-order (2+1)-dimensional Burgers equation. Through a combination of analytical techniques and numerical simulations, we aim to elucidate the conditions under which coherent structures persist, deform, or disintegrate, thereby advancing the theoretical and applied understanding of noise–nonlinearity interactions in higher-dimensional nonlinear systems.

1.1 Study Focus, Objectives, and Research Gap

This study investigates the stochastic higher-order (2+1)-dimensional Burgers equation as a framework for nonlinear wave propagation in multidimensional media under random perturbations. By combining higher-order spatial derivatives with multiplicative stochastic forcing, the model captures dynamics beyond the classical Burgers equation, including kink-type (shock-like) soliton propagation, wave-front interactions and collisions, dispersive–dissipative balance, and noise-driven energy redistribution.

The study pursues three objectives: (i) to derive and characterize N-kink soliton solutions; (ii) to assess the stability, persistence, and deformation of these coherent structures under varying multiplicative white-noise intensities; and (iii) to determine how key parameters (such as effective viscosity, wave amplitude, and noise strength) govern coherence loss and waveform distortion. The methodology integrates exact-solution techniques (notably the singular manifold method and Cole–Hopf–type transformations) with high-fidelity numerical simulations to validate theoretical predictions and resolve noise-induced effects on wave evolution.

Despite extensive work on Burgers-type models, the stochastic behavior of higher-order (2+1)-dimensional generalizations with multiplicative noise remains underdeveloped. Prior studies largely emphasize deterministic or lower-dimensional cases, where front formation and interaction mechanisms are well established [11,12,13,14,15], or stochastic soliton models that include multiplicative noise without explicitly accounting for higher-order spatial corrections and multidimensional coupling [19,20,21,28,30,31,32]. As a result, how multiplicative noise interacts with higher-order spatial structure (particularly its potential to modulate, deform, or destabilize kink solutions) has not been systematically examined. This paper addresses this gap by analyzing how multiplicative stochastic forcing alters the evolution, robustness, and coherence of kink families in a higher-order Burgers setting, with implications for noise-tolerant wave transport in plasma physics, spin-based systems, and nonlinear optical media.

Structure of the paper: Section 2 formulates the problem by presenting the governing equation and applying a wave transformation that recasts the stochastic higher-order (2+1)-dimensional Burgers equation into a form suitable for analysis. Section 3 introduces the WU system as a canonical chaotic model and discusses its relevance to stochastic spin-dynamics modeling. Section 4 derives exact solutions for the deterministic counterpart using the singular manifold method and the multiple-kink wave approach. Section 5 examines the effects of key parameters—especially noise intensity and chaotic perturbations—on soliton dynamics, supported by high-resolution numerical simulations and visualizations. Section 6 concludes the study and identifies directions for future research in stochastic nonlinear wave dynamics.

2 Stochastic higher-order (2+1) Burgers equation

The stochastic higher-order (2+1)-dimensional Burgers equation is a nonlinear stochastic partial differential equation (SPDE) that plays a vital role in modeling complex fluid dynamics, particularly in scenarios involving turbulence, shock formation, energy dissipation, and random external influences. It generalizes the classical one-dimensional Burgers equation by introducing two spatial dimensions and one temporal dimension, along with higher-order derivative terms and stochastic forcing. These extensions provide a more comprehensive and realistic framework for capturing the evolution of velocity fields in two-dimensional viscous flows influenced by both deterministic dynamics and stochastic perturbations. The incorporation of viscosity introduces energy dissipation, while the stochastic term accounts for random fluctuations that naturally arise in many physical systems. The equation's nonlinear, dissipative, and stochastic characteristics allow it to describe intricate phenomena such as the formation and interaction of shock-like structures, the transition to turbulent flow, and the influence of noise on energy transport and dissipation mechanisms. The higher-order terms enable finer control over the modeling of steep gradients and small-scale structures, which are essential in accurately capturing turbulence and shock wave behavior. The stochastic higher-order (2+1) Burgers

equation is as follows

$$M_t = 4M_{xxx} + 12NM_{xx} + 12N_xM_x + 12N^2M_x + \sigma MW_t,$$
$$M_x = N_y. \tag{1}$$

where $M(x,y,t)$ and $N(x,y,t)$ are the components of the velocity field, t denotes time, and subscripts represent partial derivatives. The parameter σ represents the intensity of the stochastic forcing, W_t denotes time white noise, σMW_t and the noise is interpreted in the Itô sense to ensure a mathematically rigorous treatment of multiplicative noise. This formulation generalizes the deterministic Burgers equation by allowing the noise amplitude to scale with the solution, introducing a multiplicative stochastic component.

The stochastic higher-order $(2+1)$ Burgers equation has wide-ranging applications in science and engineering. In fluid dynamics, it serves as a simplified yet powerful model for understanding turbulence, energy cascade, and shock dynamics (offering insights relevant to the study of the Navier–Stokes equations). In applied mathematics and computational physics, it is frequently used as a benchmark problem to evaluate numerical schemes developed for nonlinear and stochastic PDEs. Beyond fluid mechanics, the stochastic higher-order $(2+1)$ Burgers equation has found wide applicability in various scientific and engineering domains. In acoustics, it is employed to model nonlinear sound wave propagation, while in traffic flow theory, it captures spatiotemporal variations in vehicle density and velocity. In plasma physics, it aids in exploring nonlinear wave interactions and energy dissipation in magnetized plasmas. Due to its analytical tractability in certain cases, the equation also plays a central role in theoretical studies related to soliton dynamics, integrability, and perturbation analysis. Furthermore, its close relationship with the Kardar–Parisi–Zhang (KPZ) equation makes it a powerful tool for investigating interface growth, pattern formation, and surface roughening phenomena. The equation's rich mathematical structure and physical relevance not only enhance our understanding of the interplay between nonlinear convection, diffusion, and stochastic forcing but also make it a valuable benchmark for the development and testing of numerical methods for SPDEs.

2.1 Wave transformation of the stochastic higher-order (2+1)-dimensional Burgers equation

The wave equation corresponding to the stochastic higher-order $(2+1)$-dimensional Burgers equation (1) is derived through the application of the following wave transformation:

$$M(x,y,t) = m(x,y,t)e^{\left[\sigma W(t) - \frac{\sigma^2 t}{2}\right]},$$
$$N(x,y,t) = n(x,y,t)e^{\left[\sigma W(t) - \frac{\sigma^2 t}{2}\right]}. \tag{2}$$

where the functions $m(x,y,t)$ and $n(x,y,t)$ are considered deterministic, we obtain

$$\begin{aligned} M_t &= (m_t + m(\sigma W_t))\, e^{\left[\sigma W(t) - \frac{\sigma^2 t}{2}\right]}, \\ M_x &= m_x e^{\left[\sigma W(t) - \frac{\sigma^2 t}{2}\right]}, \\ M_{xx} &= m_{xx} e^{\left[\sigma W(t) - \frac{\sigma^2 t}{2}\right]}, \\ M_{xxx} &= m_{xxx} e^{\left[\sigma W(t) - \frac{\sigma^2 t}{2}\right]}, \\ N_y &= n_y e^{\left[\sigma W(t) - \frac{\sigma^2 t}{2}\right]}. \end{aligned} \tag{3}$$

By inserting Equation (2) into Equation (1) using Equation (3), we have

$$\begin{aligned} m_t - 4m_{xxx} - 12(n m_{xx} + n_x m_x) e^{\left[\sigma W(t) - \frac{\sigma^2 t}{2}\right]} \\ - 12n^2 m_x \left(e^{\left[\sigma W(t) - \frac{\sigma^2 t}{2}\right]}\right)^2 = 0, \\ m_x = n_y. \end{aligned} \tag{4}$$

Given that $W(t)$ represents the Brownian white noise function, the expectation of both sides of Equation (4) is taken to obtain

$$\begin{aligned} m_t - 4m_{xxx} - 12(n m_{xx} + n_x m_x) e^{-\sigma^2 t/2}\, \mathbb{E}\left(e^{\sigma W(t)}\right) \\ - 12n^2 m_x \left(e^{-\sigma^2 t/2}\, \mathbb{E}\left(e^{\sigma W(t)}\right)\right)^2 = 0, \\ m_x = n_y. \end{aligned} \tag{5}$$

As $W(t)$ is a Gaussian process,

$$E\left(e^{-\frac{\sigma}{2}W(t)}\right) = e^{\frac{\sigma^2}{8}t},$$

Equation (5) can therefore be expressed as

$$m_t + 4m_{xxx} - 12nm_{xx} - 12n_x m_x = 0, \quad y = m. \tag{6}$$

Representing the deterministic higher-order $(2+1)$-dimensional Burgers equation, Equation (6) can be reformulated using the following transformation:

$$y = m_n. \tag{7}$$

By substituting the potential Equation (7) into Equation (6), the latter can be transformed into

$$n_{ty} = n_{xxxy} + 12n_x n_{xxy} + 12n_{xx} n_{xy} + 12n_x^2 n_y. \tag{8}$$

3 WG System

The WG system is a three-dimensional quadratic autonomous dynamical system, recently proposed by Wu and Guo [33,34], and is known to exhibit pronounced chaotic behavior. In this paper, chaotic motion is

introduced as a stochastic excitation to examine its interaction with the system's intrinsic nonlinear dynamics. Chaotic motion (often more irregular than deterministic chaos) has the notable property that any square-integrable functional admits a Wiener–Itô chaos expansion. This representation motivates the use of the process W(t) as a mathematically tractable stochastic driver within chaotic-system modeling. The WG system is described by the following coupled first-order nonlinear differential equations:

$$\frac{df}{dt} = \alpha(f-g),\ \frac{dg}{dt} = f-\beta g+h,\ \frac{dh}{dt} = f-g^2-\gamma h,$$

where $f(t), g(t)$ and $h(t)$ denote time-dependent state variables. The system admits a broad spectrum of chaotic responses, which can be further intensified in the presence of stochastic perturbations induced by chaotic motion. A representative chaotic attractor is presented in Fig. 1, obtained for the initial conditions:

$$a = 0.5, \quad \beta = 0.15, \quad \gamma = 0.7,$$
$$f(0) = 0.02, \quad g(0) = 0.01, \quad h(0) = 0.05.$$

These simulations alter the attractor geometry and amplify the system's sensitivity to initial conditions. The resulting stochastic–chaotic coupling is evident in phase-space projections onto the $f-g$, $f-h$, and $g-h$ planes, as well as in the full three-dimensional trajectories. From the perspective of chaotic-system modulation, the results underscore the significance of stochastic effects and support the role of chaotic motion as a fundamental stochastic driver in nonlinear dynamical modeling. The chaotic dynamics of the WG system were examined through numerical simulations implemented in MATLAB using the ode45 solver. The computational analysis produced comprehensive visualizations, including time series of the state variables f(t), g(t), and h(t); two-dimensional phase portraits in the $f-g$, $f-h$, and g-h planes; and the associated three-dimensional attractor in $f-g-h$ space. Simulations were performed with the initial conditions $f(0) = 0.02$, $g(0) = 0.1$, and $h(0) = 0.05$ to ensure reproducibility and facilitate consistent comparison across runs.

The resulting time series exhibit irregular, aperiodic oscillations that are characteristic of chaotic behavior. Consistently, the phase portraits display intricate, non-repeating trajectories that neither converge to equilibria nor settle onto limit cycles, thereby confirming strong sensitivity to initial conditions. When stochastic excitation in the form of chaotic motion is introduced, the three-dimensional attractor undergoes observable topological modifications and the trajectories become more unpredictable. Nevertheless, these perturbations do not eliminate the underlying chaotic character of the system.

Overall, the simulations highlight the interplay between deterministic nonlinearity and stochastic forcing in shaping complex dynamics. The pronounced dependence on initial conditions (where small variations can yield markedly different long-term outcomes) reflects the butterfly effect and underscores the need for precise documentation of initial states in numerical studies. Given the persistence of chaotic structure under stochastic input, the WG system provides a suitable platform for investigating noise-driven chaotic dynamics.

3.1 Stochastic Modeling of Spin Dynamics via the Higher-Order (2+1)-Dimensional Burgers Equation

The stochastic higher-order (2+1)-dimensional Burgers equation constitutes a rigorous analytical framework for the study of nonlinear dynamical systems operating under random perturbations, and it is particularly well suited for contextualizing the chaotic dynamics exemplified by WG system. In such settings, spin-like state variables may exhibit pronounced sensitivity to intrinsic fluctuations and exogenous noise, thereby promoting transitions from regular oscillatory regimes to aperiodic, fully developed chaos. The incorporation of multiplicative stochastic forcing together with higher-order derivative contributions enriches the governing model, enabling a more faithful representation of dispersive–dissipative balance and nonlocal corrective effects that are often suppressed in lower-order deterministic formulations. Consequently, this extended equation provides a principled basis for analyzing how distinct noise sources (thermal, quantum, or environmental) modify stability margins, degrade coherence, and reshape the long-time evolution of nonlinear wave forms and associated dynamical invariants.

Within the specific context of WG-type dynamics used to model spin trajectories, this stochastic higher-order PDE perspective is especially pertinent because irregular state excursions can diminish energetic efficiency, disrupt phase synchrony, and undermine the robustness of coherent (including quantum) states (limitations that are central in spintronics and quantum information processing). The framework supports systematic investigation of critical nonlinear phenomena, including bifurcation structure, noise-triggered transitions to chaos, and noise-induced pattern formation in wave-like responses. Moreover, it enables statistical characterization of system behavior over extended timescales through ensemble measures (e.g., moments, correlation functions, and probability distributions), thereby clarifying the dual role of noise as both a destabilizing agent and a mechanism capable of precipitating emergent order. By embedding time-dependent interaction effects (such as magnetic coupling terms) into a unified stochastic higher-order

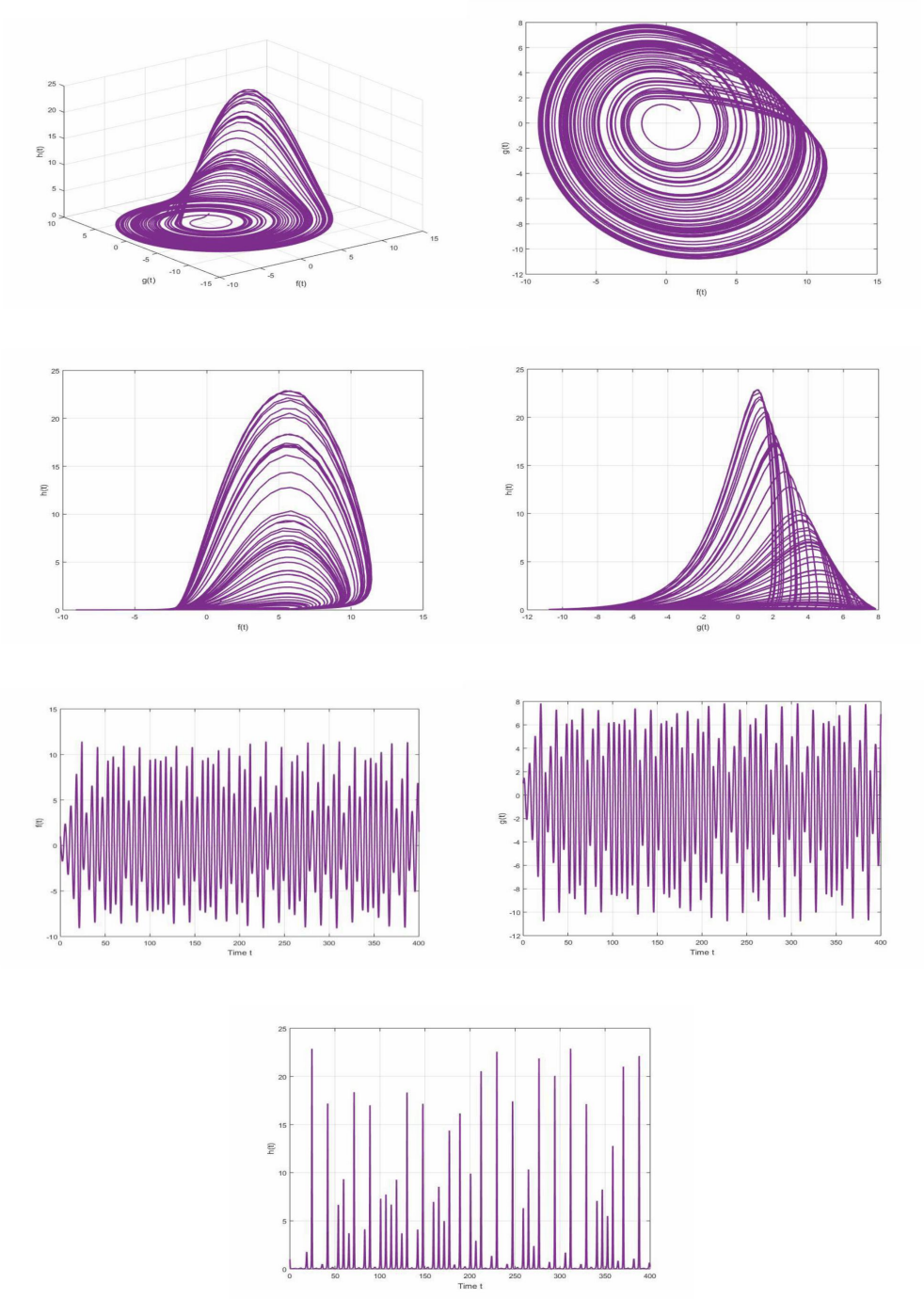

Fig. 1: Simulation of WG system dynamics via MATLAB's ode45 solver. The graphic illustrates time series for $f(t)$, $g(t)$, and $h(t)$, 2D-phase portraits $(f-g, f-h, g-h)$, and 3D of ($f-g-h$) space. The simulations have the parameters $\alpha = 0.2$, $\beta = 0.15$, $\gamma = 0.7$, and initial conditions $f_0 = 0.02$, $g_0 = 0.01$, $h_0 = 0.05$. (a) the 3D in $f-g-h$ space, (b) 2D phase projection in the g-h plane, (c) 2D phase projection in the $f-h$ plane, and (d) 2D phase projection in the $f-g$ plane, and (e) time series of $h(t)$, $g(t)$, and $f(t)$.

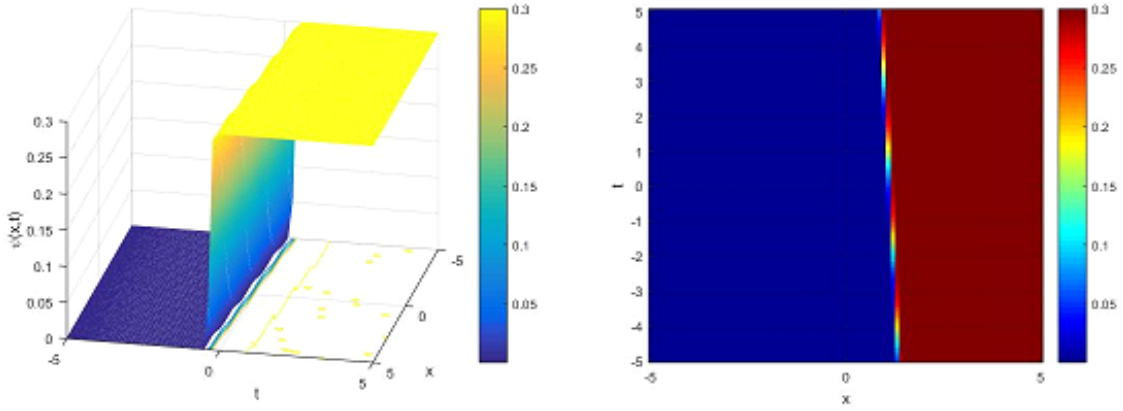

Fig. 2: illustrates the evolution of the kink-shaped soliton solution described by Equation (30). (a) provides a three-dimensional representation, whereas (b) shows the corresponding density plot. Both visualizations were obtained using the parameter values $\sigma = 0$, $k_1 = 2$, and $r_1 = 0.3$. These plots clearly capture the characteristic spatial structure and propagation dynamics of the kink-shaped soliton

continuum description, one obtains a physically grounded and mathematically coherent route to interpret chaotic spin evolution and to inform the development of control strategies aimed at mitigating (or, where advantageous, exploiting) chaos in next-generation spin-based and quantum technologies.

3.2 Wiener-Driven Trajectories based on WG system and Their Embedding into a Stochastic Higher-Order (2+1)-Dimensional Burgers Framework

In the stochastic formulation considered here, the evolution of WU-type state variables is modeled as an Itô diffusion driven by a Wiener process. For completeness, we recall the basic definitions. A real-valued Wiener process $\{W_t\}_{t\geq 0}$ is a stochastic process satisfying: (i) $W_0 = 0$ almost surely; (ii) it has independent increments, meaning that for $0 \leq t_0 < t_1 < \cdots < t_n$, the random variables

$$W_{t_1} - W_{t_0},\ W_{t_2} - W_{t_1},\ \ldots,\ W_{t_n} - W_{t_{n-1}}$$

are mutually independent; (iii) it has Gaussian increments with

$$W_{t+s} - W_t \sim \mathcal{N}(0,s) \quad \text{for all } s \geq 0;$$

and (iv) its sample paths $t \mapsto W_t(\omega)$ are almost surely continuous (while being nowhere differentiable). A trajectory "driven by a Wiener process" is then defined through an Itô SDE of the form

$$dX_t = a(X_t,t)\,dt + b(X_t,t)\,dW_t,$$

where X_t is the stochastic process of interest, a is the drift coefficient, and b is the diffusion (noise) coefficient. The solution can be written formally as

$$X_t = X_{t_0} + \int_{t_0}^{t} a(X_s,s)\,ds + \int_{t_0}^{t} b(X_s,s)\,dW_s,$$

where the second term on the right-hand side is an Itô stochastic integral with respect to the Wiener process. In this sense, the random trajectory $t \mapsto X_t$ is "driven" by the Wiener process W_t.

We outline a principled procedure by which an effective Wiener process may be derived from a deterministic WG system through a diffusion approximation. Consider the classical Rössler flow $\varphi_t(x_0)$ generated by

$$\frac{df}{dt} = -g - h, \qquad \frac{dg}{dt} = f + ag, \qquad \frac{dh}{dt} = b + h(f-c),$$

with parameters (a,b,c) chosen in a chaotic regime. Let $h : \mathbb{R}^3 \to \mathbb{R}$ be a scalar observable (for example, $\varphi(f,g,h) = f$), and define the centered signal

$$\zeta(t) = \varphi(\phi_t(x_0)) - \bar{\varphi}, \qquad \bar{\varphi} = \lim_{T\to\infty} \frac{1}{T}\int_0^T \varphi(\phi_s(x_0))\,ds,$$

where $\bar{\varphi}$ denotes the invariant (long-time) mean, estimated numerically after discarding transients. For

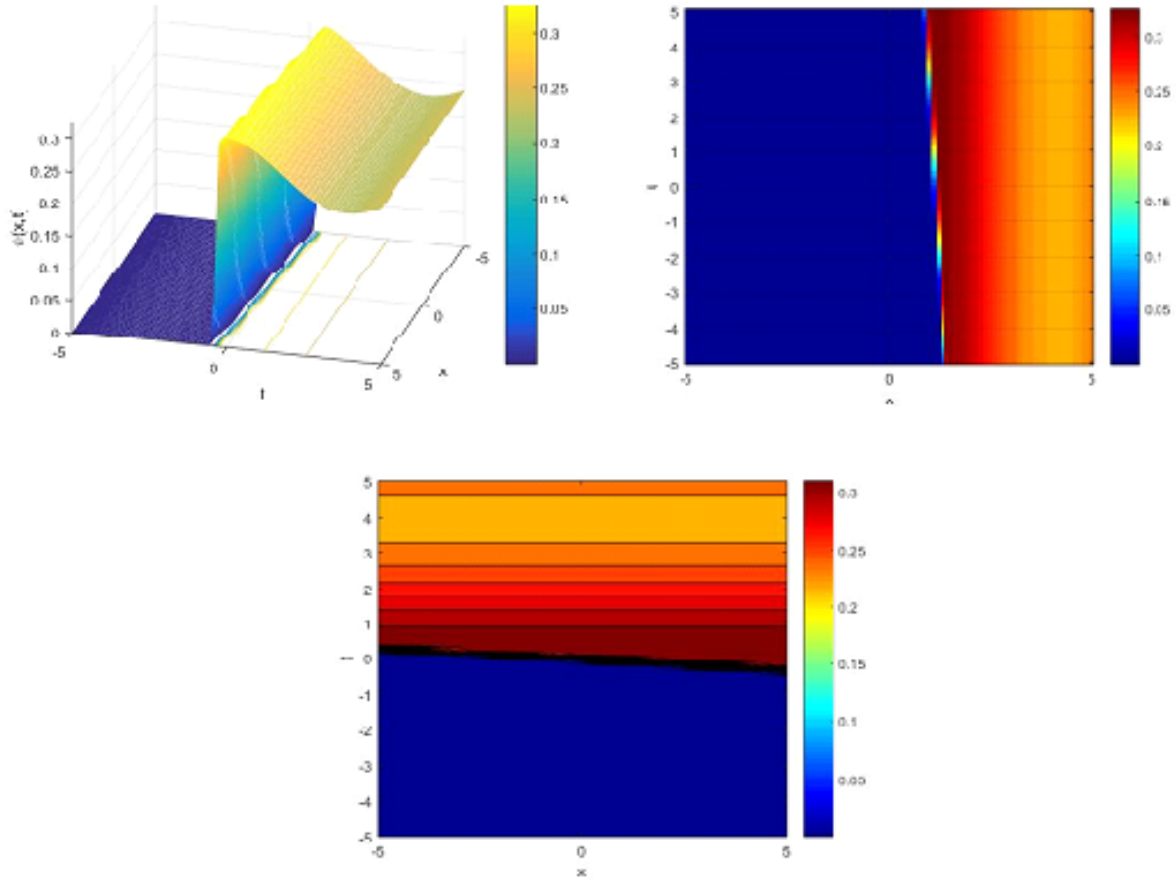

Fig. 3: presents the non-flat kink-shaped soliton solution derived from Equation (30). (a) shows the three-dimensional surface plot, (b) depicts the corresponding density plot, and (c) displays the heatmap. All visualizations were generated using the parameters $\sigma = 0.3$, $k_1 = 2$, and $r_1 = 0.3$. These results demonstrate the influence of a small, nonzero noise parameter (σ) on the structure and temporal evolution of the kink-shaped soliton.

chaotic Rössler dynamics, $\zeta(t)$ typically exhibits sufficiently rapid decay of correlations (mixing) so that long-time accumulated fluctuations behave diffusively. This motivates the construction of a rescaled integrated process

$$W_T(t) = \frac{1}{\sqrt{T}} \int_0^{tT} \zeta(s)\, ds, \qquad t \geq 0,$$

which serves as a Brownian-motion candidate extracted from the deterministic chaotic signal. Under a weak invariance principle (functional central limit theorem) for mixing flows, the process $W_T(\cdot)$ converges in distribution, as $T \to \infty$, to a Wiener process with an effective diffusion coefficient. More precisely, one expects

$$W_T(\cdot) \Rightarrow \sqrt{D} B(\cdot),$$

where $B(t)$ is a standard Wiener process and $D > 0$ is determined by the autocovariance structure of ζ through a Green–Kubo-type relation,

$$D = 2 \int_0^{\infty} textcov(\zeta(0), \zeta(s))\, ds.$$

In computational practice, this limit is assessed by verifying that the increments $W_T(t + \Delta) - W_T(t)$ are approximately Gaussian with variance proportional to Δ, and that $textVar[W_T(t)] \approx Dt$ over the time window of interest. Having obtained W_T, one may normalize it via

$$\widetilde{W}_T = \frac{1}{\sqrt{D}} W_T$$

so that $\widetilde{W}_T$ approximates a standard Wiener process. This provides a mathematically coherent mechanism by which deterministic chaotic WG-type dynamics can be represented, at coarse scales, as an effective Brownian driver suitable for inclusion in Itô stochastic models and, in particular, for embedding into stochastic PDE

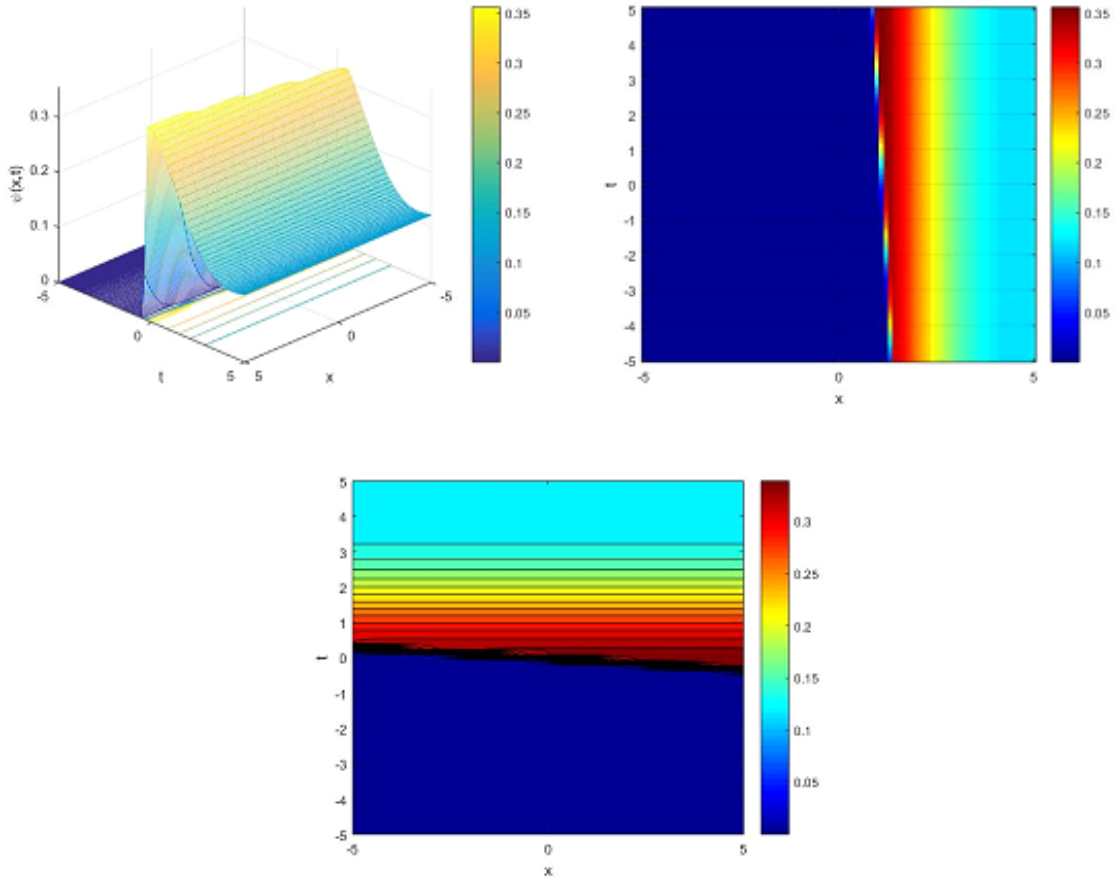

Fig. 4: presents the non-flat kink-shaped soliton solution derived from Equation (30). (a) shows the three-dimensional surface representation, (b) illustrates the corresponding density plot, and (c) depicts the heatmap. All visualizations were generated using the parameters $\sigma = 0.6$, $k_1 = 2$, and $r_1 = 0.6$. The results emphasize the increased structural deformation of the soliton as the noise intensity (σ) rises.

frameworks (e.g., higher-order Burgers-type equations) through noise terms of the form $\sigma(M,N,t)\,dW_t$.

4 Explicit Solutions to the Stochastic Higher-Order (2+1)-Dimensional Burgers Model

In this section, we explore explicit solutions of the stochastic higher-order (2+1)-dimensional Burgers equation, incorporating both deterministic and stochastic components as well as higher-order spatial derivatives. The analytical framework is based on a combination of the singular manifold method and leading-order analysis, extended to accommodate the stochastic and higher-order nature of the equation. This approach yields a class of exact solutions parameterized by arbitrary functions, capturing the rich nonlinear and noise-driven dynamics of the system. To further investigate wave structures, we construct multiple-kink solutions by integrating the exponential method with a generalized Cole–Hopf transformation, adapted for the stochastic context. These solutions describe nonlinear wave interactions that can evolve into sharp gradients and localized features, closely resembling shock-like structures even under the influence of stochastic perturbations. The singular manifold method serves as a systematic tool for uncovering exact solutions by leveraging the integrable structure of the extended Burgers model, while the generalized Cole–Hopf transformation linearizes the equation, allowing the stochastic and nonlinear components to be treated more tractably. The resulting kink-type solutions offer insight into the dissipative and noise-influenced mechanisms underlying wave front propagation, shock merging, and pattern formation in two-dimensional viscous media. Physically, these solutions provide a valuable basis for

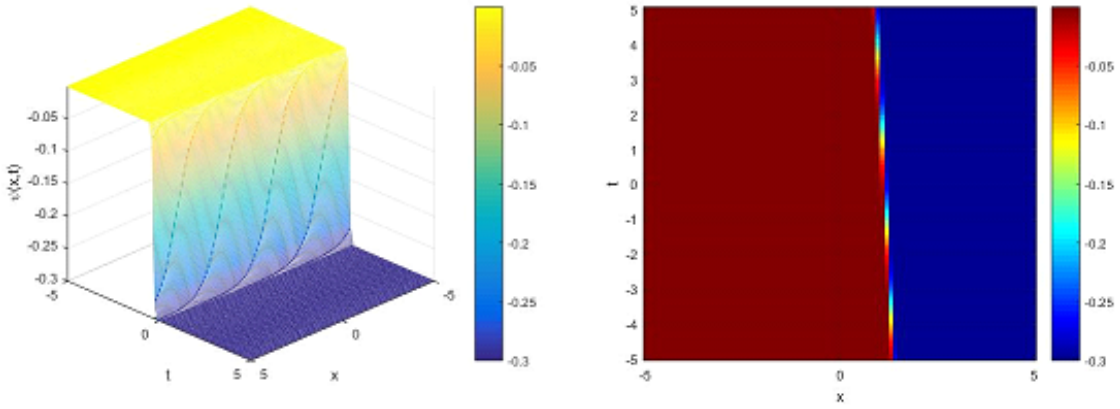

Fig. 5: illustrates the evolution of the anti–kink–shaped soliton solution described by Equation (30). (a) provides a three-dimensional representation, (b) shows the corresponding density plot. Both visualizations were generated using the parameter values$\sigma = 0$, $k_1 = 2$, and $r_1 = -0.3$. These plots clearly depict the characteristic spatial configuration and propagation dynamics of the anti–kink-shaped soliton.

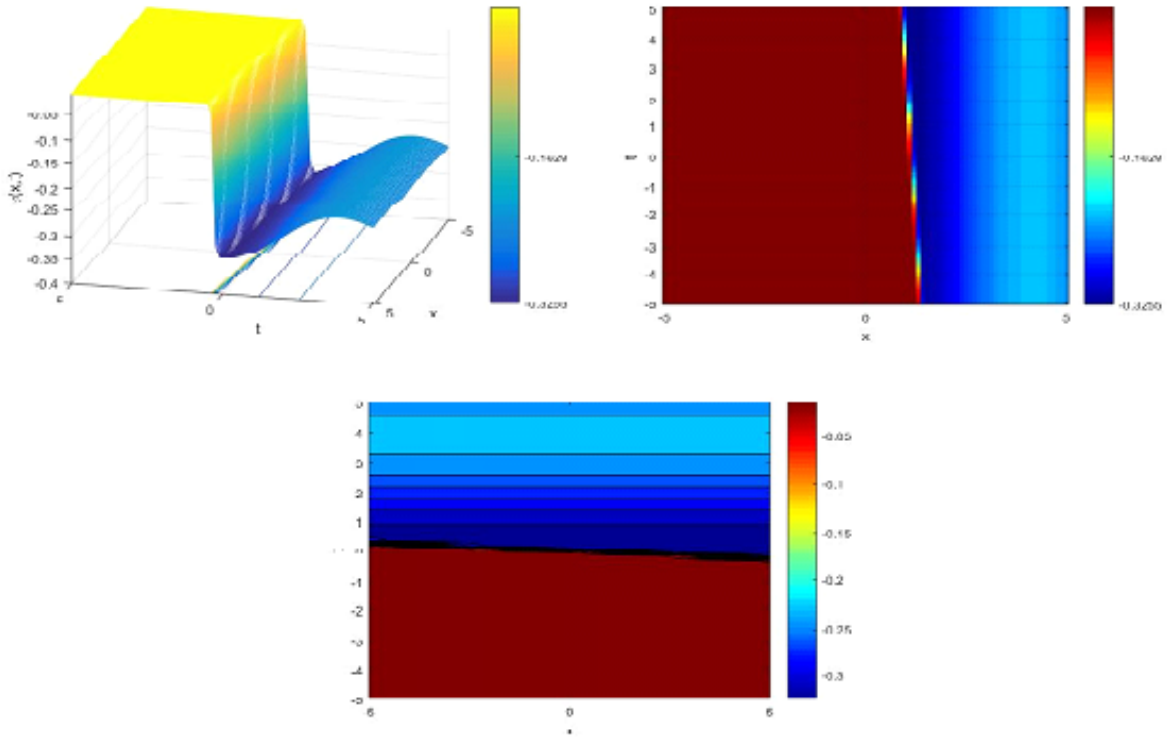

Fig. 6: presents the non-flat anti–kink-shaped soliton solution derived from Equation (30). (a) shows the three-dimensional surface plot, (b) depicts the corresponding density plot, and (c) displays the heatmap. All visualizations were generated using the parameters$\sigma = 0.3$, $k_1 = 2$, and $r_1 = -0.3$. These results demonstrate the impact of a small, nonzero noise parameter (σ) on the structure and temporal evolution of the anti–kink-shaped soliton.

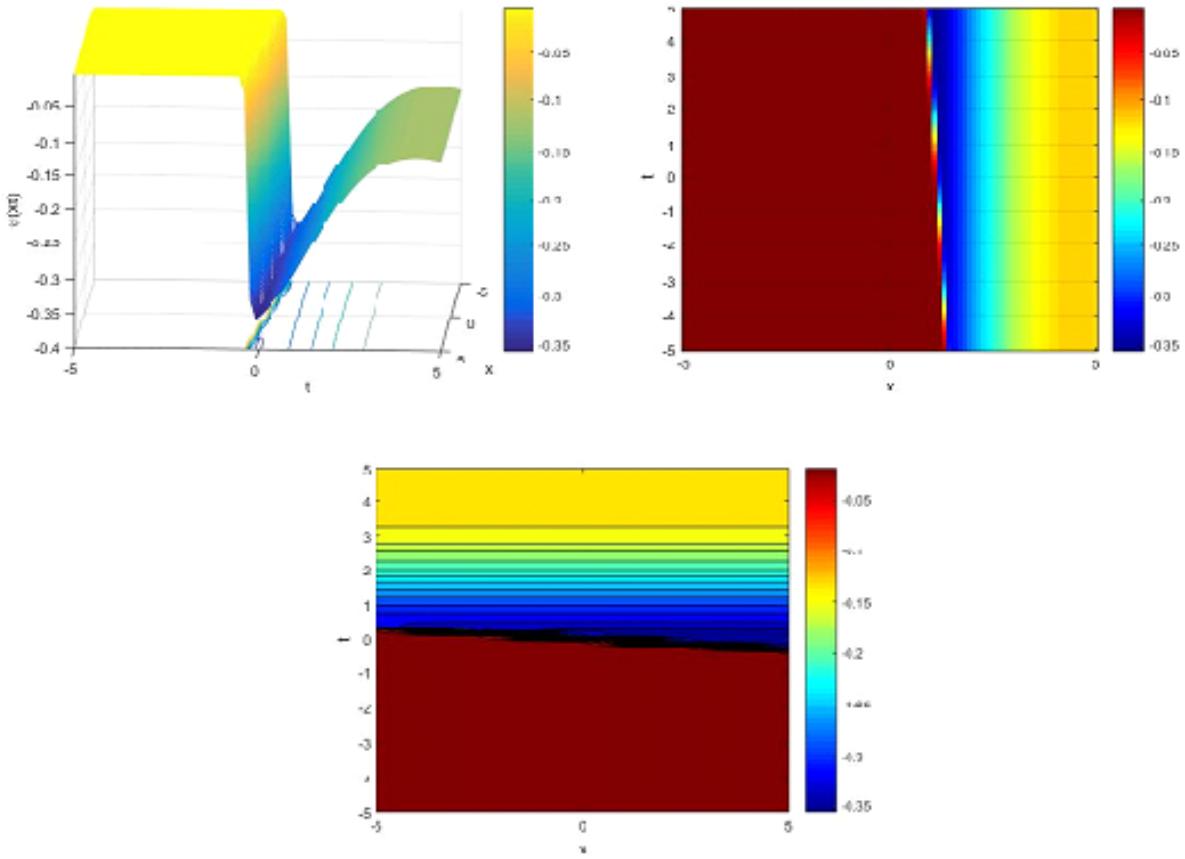

Fig. 7: presents the non-flat anti–kink-shaped soliton solution derived from Equation (30). (a) shows the three-dimensional surface representation, (b) illustrates the corresponding density plot, (c) depicts the heatmap. All visualizations were generated using the parameters$\sigma = 0.6$, $k_1 = 2$, and $r_1 = -0.3$. The results highlight the increased structural deformation of the anti–kink soliton as the noise intensity (σ) increases.

understanding the interplay between nonlinearity, dispersion, and stochastic forcing in fluid systems, and they serve as analytical benchmarks for evaluating numerical solvers developed for stochastic partial differential equations. Altogether, the synthesis of singular manifold analysis with the exponential–Cole–Hopf framework deepens the theoretical understanding of the stochastic higher-order (2+1)-dimensional Burgers equation, underscoring its applicability to a wide range of complex dynamical phenomena.

4.1 Singular Manifold Techniques

By applying the singular manifold method in conjunction with leading-order analysis, the Painlevé expansion of Equation (6) can be truncated to obtain a simplified form, expressed as

$$n = \frac{\varphi_x}{\varphi} + m_1, \qquad m = \frac{\varphi_y}{\varphi} + n_1. \tag{9}$$

with φ is the singular manifold, and $\{M_1, N_1\}$ is an arbitrary solution of Equation (6), and φ satisfies

$$\varphi_t = \varphi_{xxx} + 4\varphi_x\varphi_{xx} + 12\varphi_x^2 n_1. \tag{10}$$

Taking the trivial solution, $m_1 = 0, n_1 = 0$, Cole–Hopf type transformation or hetero–Bäcklund fractional transformation

$$m = \frac{\varphi_x}{\varphi}. \tag{11}$$

Equation (11), where φ satisfies $\varphi_t = \varphi_{xxx}$ is obtained for Equation (10).

Taking another initial solution, $y_1 = \varphi_y, m_1 = \varphi_x$, then

$$m = \frac{\varphi_x}{\varphi} + \varphi_x, \tag{12}$$

we obtain another new auto–Bäcklund fractional transformation for Equation (6) with φ satisfying

$$\varphi_t = 4\varphi_{xxx} + 12\psi\,\varphi_{xx} + 12\psi_x\,\varphi_x + 12\psi^2\,\varphi_x, \quad \varphi_x = \psi_y. \tag{13}$$

It is noteworthy that this equation simultaneously satisfies both Equations (6) and (8), demonstrating its consistency within the established framework. The singular manifold method serves as a powerful analytical tool for deriving exact solutions to nonlinear differential equations. In this work, the method is employed to construct explicit solutions by initiating the process with an appropriate seed solution. Our generalized formulation of the singular manifold equation incorporates three arbitrary functions, providing a flexible foundation for generating a wide spectrum of solution structures through suitable functional choices. It should also be noted that Equations (9) through (13) correspond directly to Equations (25) to (27) as presented in the work by Peng and Yamba [15].

4.2 Multiple-Kink Wave Solution

We now turn our attention to the multiple-kink wave solution. By selecting

$$n_i = e^{k_i x + r_i y - c_i t}, \tag{14}$$

Substituting into the linear term of Equation (8) yields the dispersion relation

$$c_i = -k_i^3. \tag{15}$$

We then obtain

$$\theta_i = k_i x + r_i y + k_i^3 t. \tag{16}$$

Applying the Cole–Hopf transformation yields the multiple-kink wave solution of Equation (11) as

$$n = \ln(Rf), \tag{17}$$

and

$$m = \frac{Rf_y}{f}. \tag{18}$$

For the case of the one-kink wave solution

$$f = 1 + e^{k_1 x + r_1 y + k_1^3 t}. \tag{19}$$

By substituting this equation into Equation (8) and subsequently solving for R, we obtain $R = 1$. Therefore

$$n = \ln\left(1 + e^{k_1 x + r_1 y + k_1^3 t}\right). \tag{20}$$

The one-kink wave solution is therefore given by

$$m = \frac{r_1 e^{k_1 x + r_1 y + k_1^3 t}}{1 + e^{k_1 x + r_1 y + k_1^3 t}}. \tag{21}$$

Accordingly, the two-kink wave solution is obtained in the form

$$f = 1 + e^{\theta_1} + e^{\theta_2} + a_{12} e^{\theta_1 + \theta_2}. \tag{22}$$

By substituting this equation into Equation (17) and subsequently inserting the resulting expression into Equation (8), we obtain $R = 1$, with no phase shifts observed, $a_{12} = 0$. therefore, we obtain $a_{ij} = 0, i \le i \le j \le 3$. Accordingly, we have

$$n = \ln\left(1 + e^{k_1 x + r_1 y + k_1^3 t} + e^{k_2 x + r_2 y + k_2^3 t}\right). \tag{23}$$

Accordingly, the two-kink wave solution takes the form

$$m = \frac{r_1 e^{k_1 x + r_1 y + k_1^3 t} + r_2 e^{k_2 x + r_2 y + k_2^3 t}}{1 + e^{k_1 x + r_1 y + k_1^3 t} + e^{k_2 x + r_2 y + k_2^3 t}}. \tag{24}$$

To discuss the three-kink soliton solution, and following the same procedure as before, we obtain

$$n = \ln\left(1 + e^{k_1 x + l_1 y + 4k_1^3 t} + e^{k_2 x + l_2 y + 4k_2^3 t} + e^{k_3 x + l_3 y + 4k_3^3 t}\right). \tag{25}$$

This yields the three-kink wave solution

$$m = \frac{\psi_2}{1 + \psi_1}. \tag{26}$$

Proceeding in the same way as before, we have

$$n = \ln\left(1 + \psi_1\right) \tag{27}$$

this yields the four-kink wave solution

$$m = \frac{\psi_2 + r_4 e^{k_4 x + r_4 y + 4k_4^2 t}}{1 + \psi_1}. \tag{28}$$

where

$$\psi_1 = e^{k_1 x + r_1 y + 4k_1^2 t} + e^{k_2 x + r_2 y + 4k_2^2 t} + e^{k_3 x + r_3 y + 4k_3^2 t} + e^{k_4 x + r_4 y + 4k_4^2 t},$$

$$\psi_2 = r_1 e^{k_1 x + r_1 y + 4k_1^2 t} + r_2 e^{k_2 x + r_2 y + 4k_2^2 t} + r_3 e^{k_3 x + r_3 y + 4k_3^2 t}.$$

This is significant because the higher order (2+1)-dimensional Burgers equation (Equation (8)) admits N-kink solutions for any finite $N \ge 1$. These solutions capture the interactions among multiple nonlinear wave fronts, which may merge, split, or evolve into complex spatiotemporal structures. Each kink corresponds to a localized steep gradient or shock-like feature, and the presence of multiple such structures within a single solution underscores the equation's capacity to represent complex dynamical phenomena, including wave front collisions, shock coalescence, and pattern formation in dissipative systems. From a physical perspective, N-kink configurations are especially relevant in contexts where several discontinuities or sharp transitions occur concurrently such as turbulent fluid flows, traffic congestion modeling, acoustic shock propagation, and interface dynamics. The interaction

dynamics of these kinks provide valuable insight into mechanisms of energy redistribution and the emergence of ordered patterns within nonlinear media. Mathematically, the existence of such multi-kink solutions highlights the structural richness of the Burgers equation?s solution space. These solutions not only offer exact benchmarks for testing the accuracy and robustness of numerical solvers but also serve as meaningful initial conditions for investigating stability properties and long-term system behavior. Based on the results derived, the general form of the kink solutions can be expressed as

$$n = \ln\left(1+\sum_{i=1}^{N} e^{k_i x + r_i y + k_i^3 t}\right), \qquad m = \frac{\sum_{i=1}^{N} r_i e^{k_i x + r_i y + k_i^3 t}}{1+\sum_{i=1}^{N} e^{k_i x + r_i y + k_i^3 t}}. \tag{29}$$

4.3 Numerical treatment

Let $(M,N)(x,y,t)$ denote the velocity-field components governed by the stochastic higher-order (2+1)-dimensional Burgers SPDE, where the stochastic forcing is multiplicative with intensity σ and is explicitly interpreted in the Itô sense. A standard numerical treatment begins by discretizing a rectangular spatial domain $\Omega = [x_{\min}, x_{\max}] \times [y_{\min}, y_{\max}]$ on a uniform mesh (x_i, y_j) and approximating spatial derivatives in (1) via consistent finite-difference stencils (central differences for first/second derivatives; repeated application or dedicated stencils for higher-order derivatives). Writing the semi-discrete system abstractly as an Itô SDE in time,

$$dU = F(U)\,dt + \sigma\, G(U)\,dW_t$$

(with U stacking the grid values of M,N), an Itô-consistent time integrator such as Euler–Maruyama yields the update

$$U^{n+1} = U^n + \Delta t\, F(U^n) + \sigma\, G(U^n)\,\Delta W^n,$$

where $\Delta W^n \sim \mathcal{N}(0,\Delta t)$.

In parallel, the manuscript's deterministic reduction obtained by taking expectation and applying the potential transformation provides a validation pathway: numerical solutions of the SPDE (or of its expected/potential form) should converge under refinement and reproduce the deterministic limit as $\sigma \to 0$.

In the manuscript's computational workflow, "numerical simulations" primarily quantify how multiplicative noise deforms analytically constructed soliton profiles: the kink-shaped solution (Eq.(30)) and the two-kink solution (Eq.(31)) are evaluated on a spatiotemporal grid while varying σ (notably $\sigma = 0, 0.3, 0.6$) and fixed parameter sets, e.g., $(k_1, r_1) = (2, -0.3)$ for anti-kinks and $(k_1, k_2, r_1, r_2) = (-3, 4, 2, 5)$ for two-kinks; the resulting fields are then rendered as 3D surfaces/density maps/heatmaps to assess coherence degradation with increasing σ. Separately, the paper integrates the Rössler system using MATLAB's `ode45` with parameters $(a,b,c) = (0.2, 0.2, 5.7)$ and initial state $(f_0, g_0, h_0) = (1,1,1)$, producing time series and phase portraits as numerical evidence of chaotic dynamics.

5 Simulation Results of Wave Pattern Dynamics

This section presents the numerical analysis of the stochastic higher-order (2+1)-dimensional Burgers equation, aiming to validate the theoretical N-kink wave solutions derived previously and to explore the rich dynamical behaviors that emerge under various conditions. Through systematic variation of initial configurations, system parameters, and the number of interacting wave fronts, the simulations reveal a broad spectrum of spatiotemporal patterns, including well-defined kink collisions, evolving wave structures, and interference effects. Accurate time integration was ensured using high-precision numerical solvers, and the results are displayed via time-series data, phase-space trajectories, and space-time contour plots. These simulations highlight several fundamental characteristics, such as the persistence and interaction of localized wave fronts, the formation of shock-like gradients, and the modulation of wave amplitudes and velocities in response to changes in viscosity, noise intensity, and initial wave profiles. The influence of additive white noise was closely examined, demonstrating that at low noise amplitudes, perturbations in phase, amplitude, and velocity remain minimal. However, increased noise levels significantly distort the structure of solitary and kink-type solutions, eventually leading to the degradation and destabilization of coherent wave forms. Kink solitons, defined as topological wave structures characterized by step-like transitions between distinct asymptotic states, play a fundamental role in numerous nonlinear systems. They arise naturally in fields such as condensed matter physics (e.g., magnetic domain walls, dislocations in crystal lattices, and Josephson junctions), spintronics (modeling spin-transfer torque and magnetization reversal), nonlinear optics, and field theory. The present simulations underscore the sensitivity of these structures to stochastic perturbations in the higher-order Burgers framework. While low-intensity noise allows for partial preservation of soliton integrity, strong stochastic forcing disrupts both amplitude and phase coherence, leading to structural disintegration beyond a critical noise threshold. The robustness of these solutions was also shown to depend on specific system parameters, such as k_i and r_i, suggesting that careful parameter tuning can enhance stability in noisy environments. These findings contribute to a deeper understanding of the interplay between nonlinearity and stochasticity, and offer valuable insights for the design of noise-resilient soliton-based systems in applied physics and engineering contexts. Future investigations should extend the analysis to more complex

noise models (including colored and multiplicative noise) and explore a wider parameter space to fully characterize the dynamics of noise-induced transitions and soliton longevity.

Based on the results derived in equation (21) and applying the relationship established in equation (2) the corresponding expressions for

$$M(x,y,t) = \frac{r\,e^{kx+ry+4k^3t}}{1+e^{kx+ry+4k^3t}}\,e^{\sigma W(t)-\frac{1}{2}\sigma^2 t}. \qquad (30)$$

The impact of multiplicative noise on the one-kink soliton solution of the stochastic higher-order (2+1)-dimensional Burgers equation was investigated through detailed numerical simulations. The analysis focused on evaluating soliton stability under varying noise intensities. As a reference, Figure 2 depicts the deterministic soliton profile obtained from Equation (30) with zero noise intensity ($\sigma = 0$), serving as a baseline for comparison. Figures 3 and 4 illustrate the soliton's evolution under weak ($\sigma = 0.3$) and moderate ($\sigma = 0.6$) noise, respectively. At lower noise levels, the soliton retains its structural coherence, exhibiting only minor fluctuations in amplitude and phase. However, with increasing stochastic influence, noticeable deformations emerge, reflecting the system's growing sensitivity to external perturbations. To further explore the system's behavior, Figures 5–7 present soliton profiles generated by reversing the sign of the parameterr_1, which exhibit similar noise-dependent dynamics. All simulations were conducted with fixed parameters $k_1 = 2$ and $r_1 = 0.3$. The results indicate that while weak noise induces negligible disturbances, stronger noise intensities lead to pronounced alterations in soliton shape and, in some instances, partial loss of coherence. These observations emphasize the delicate interplay between nonlinearity, dispersion, and stochastic forcing, where the stability of solitonic structures hinges on maintaining a precise dynamical balance. This investigation highlights the dual nature of multiplicative noise in nonlinear systems: low-intensity fluctuations can be absorbed without significant disruption, whereas high-intensity noise undermines soliton stability. These insights are particularly relevant for physical systems where kink-like structures are integral, such as domain walls in condensed matter physics, spin-transfer torque devices, and signal propagation in noisy media. Additionally, the findings underline the importance of parameter tuning, especially with respect to k_1, r_1, and noise-related coefficients, to enhance the resilience of soliton-based configurations in stochastic environments.

Based on the results obtained from Equation (24) and utilizing the relationship defined in Equation (2), the corresponding expressions for M can be written as

$$M(x,y,t) = \frac{r_1 e^{k_1x+y+4\delta_1 t} + r_2 e^{k_2x+y+4\delta_2 t}}{1+e^{k_1x+y+4\delta_1 t} + e^{k_2x+y+4\delta_2 t}}\,e^{-\delta^n(t-\sigma_1 t_2)}. \qquad (31)$$

The influence of multiplicative noise on the two-kink soliton solution of the stochastic higher-order (2+1)-dimensional Burgers equation was systematically examined through extensive numerical simulations. The robustness of soliton profiles was assessed across a range of noise intensities. Figure 8 presents the deterministic two-kink solution derived from Equation (31) under noise-free conditions ($\sigma = 0$), serving as a baseline for evaluating stability. In contrast, Figures 9 and 10 illustrate the soliton's response to mild ($\sigma = 0.3$) and moderate ($\sigma = 0.6$) noise levels, respectively. Under weak stochastic influence, the two-kink soliton preserves its overall coherence, with only subtle modulations in amplitude and phase. However, as noise strength increases, the solution becomes increasingly distorted, indicating heightened sensitivity to external perturbations. Further insight is provided by Figures 11 through 13, which depict mirrored soliton configurations obtained by inverting the signs of parameters r_1 and r_2. These profiles exhibit similar noise-dependent behavior, reinforcing the observed trends. All simulations were performed using fixed parameter values $k_1 = -3, k_2 = 4, r_1 = 2$, and $r_2 = 5$. The findings confirm that while low-intensity noise introduces negligible distortions, higher noise levels substantially deform the soliton structure and can lead to a partial breakdown of coherence. These results emphasize the dual character of multiplicative noise in nonlinear dynamical systems: minor fluctuations are generally manageable, but strong stochastic forcing undermines the fine-tuned balance between nonlinearity and dispersion required for soliton persistence. This behavior has significant implications for practical systems where two-kink structures play a central role, including magnetic domain wall dynamics, spintronic devices, and signal propagation in noisy media. The simulations also highlight the necessity of careful parameter optimization (specifically involving k_1, k_2, r_1, r_2, and noise-related coefficients) to enhance the structural resilience of soliton solutions in stochastic environments.

6 Physical interpretation of the obtained solutions

The explicit kink and multi-kink solutions obtained for the stochastic higher-order (2+1)-dimensional Burgers framework admit a clear physical interpretation as shock-like coherent fronts propagating in a multidimensional dissipative medium. In this setting, the field components (e.g., $M(x,y,t)$ and $N(x,y,t)$) may be interpreted as a two-dimensional flow/transport state whose evolution is governed by the competition between nonlinear steepening, viscous smoothing, and higher-order spatial corrections. A single kink therefore represents a traveling transition layer separating two distinct asymptotic states, i.e., a localized steep gradient that is maintained by the nonlinear–dissipative balance

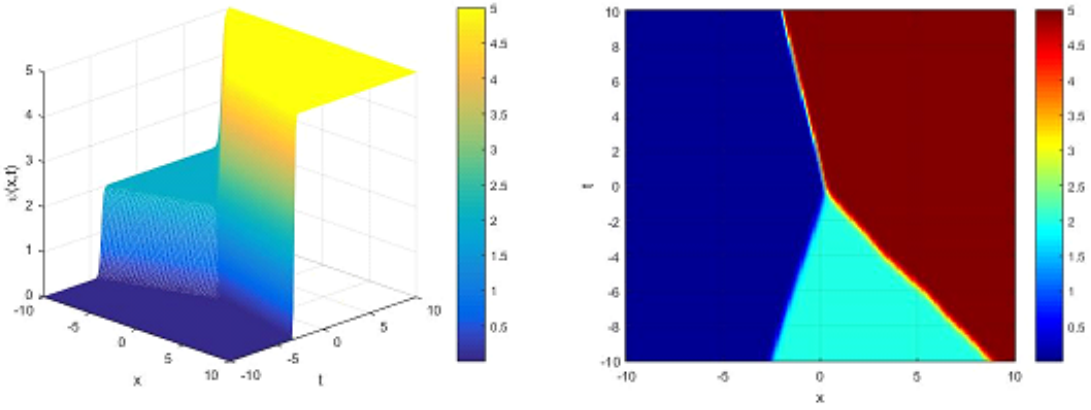

Fig. 8: illustrates the evolution of the two–kink-shaped soliton solution described by Equation (31). Subfigure (a) provides a three-dimensional representation, while subfigure (b) shows the corresponding density plot. Both visualizations were produced using the parameter values$\sigma = 0, k_1 = -3, k_2 = 4\ r_1 = 2$and $r_2 = 5$. These plots clearly depict the characteristic spatial structure and propagation dynamics of the two–kink-shaped soliton.

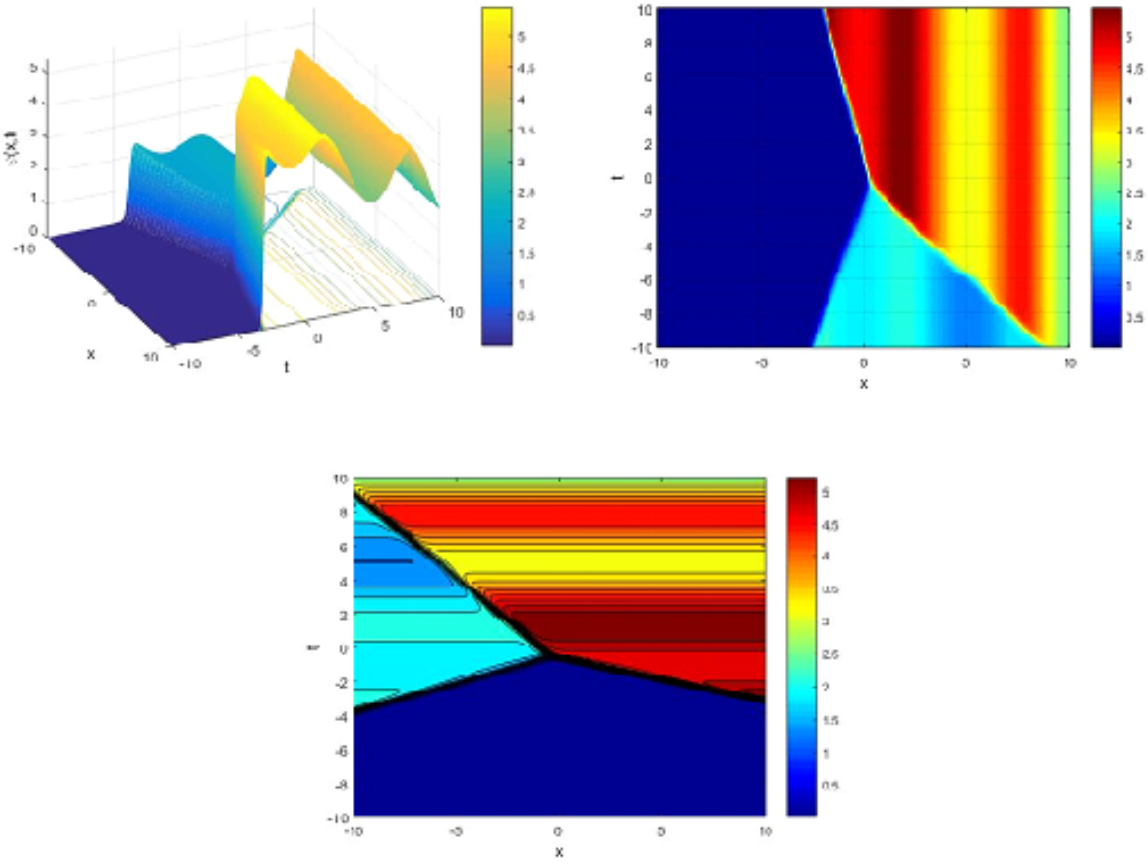

Fig. 9: presents the non-flat two–kink-shaped soliton solution derived from Equation (31). (a) shows the three-dimensional surface plot, (b) depicts the corresponding density plot, and subfigure (c) displays the heatmap. All visualizations were produced using the parameter values$\sigma = 0.3, k_1 = -3, k_2 = 4\ r_1 = 2$and $r_2 = 5$. These results illustrate the influence of a small, nonzero noise parameter (σ) on the structure and temporal evolution of the two–kink–shaped soliton.

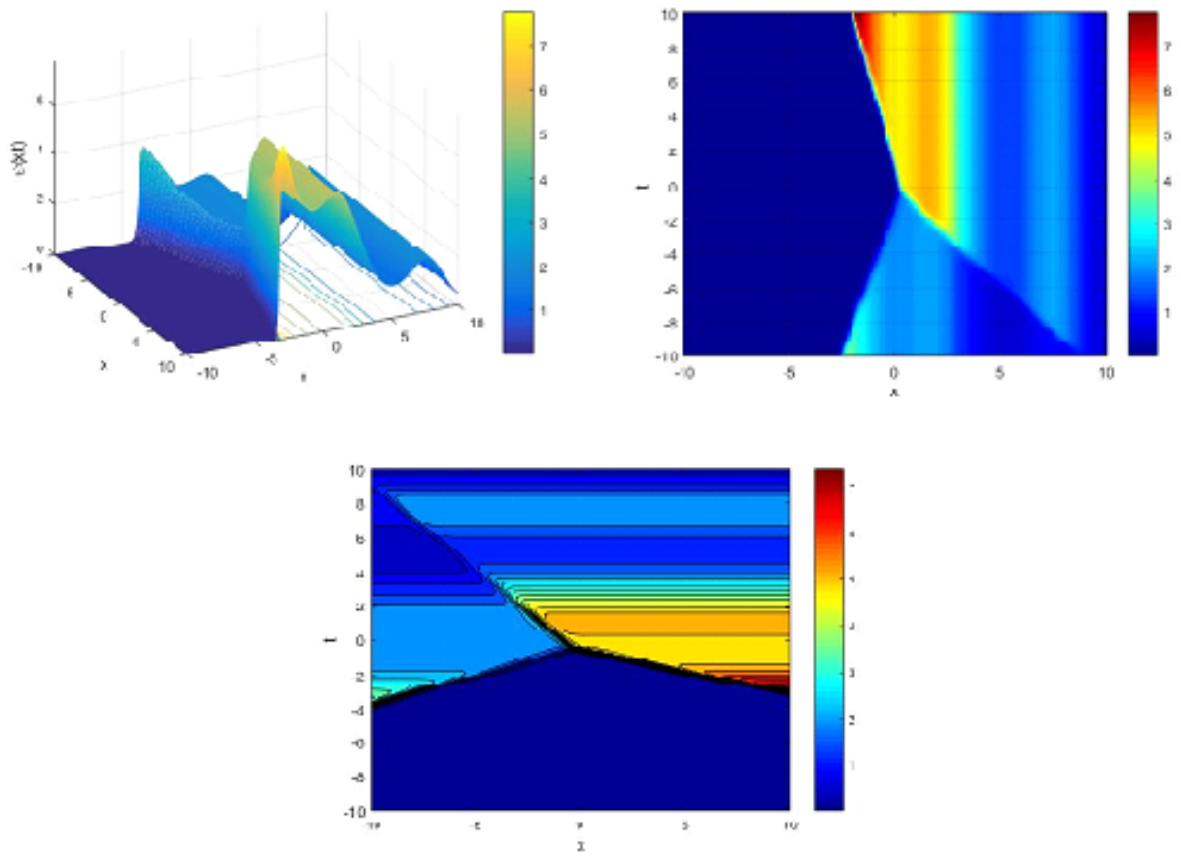

Fig. 10: presents the non-flat two–kink-shaped soliton solution derived from Equation (31). (a) shows the three-dimensional surface representation, (b) illustrates the corresponding density plot, (c) depicts the heatmap. All visualizations were produced using the parameter values$\sigma = 0.6$, $k_1 = -3$, $k_2 = 4$ $r_1 = 2$and $r_2 = 5$. The results highlight the enhanced structural deformation of the two–kink soliton as the noise intensity (σ) increases.

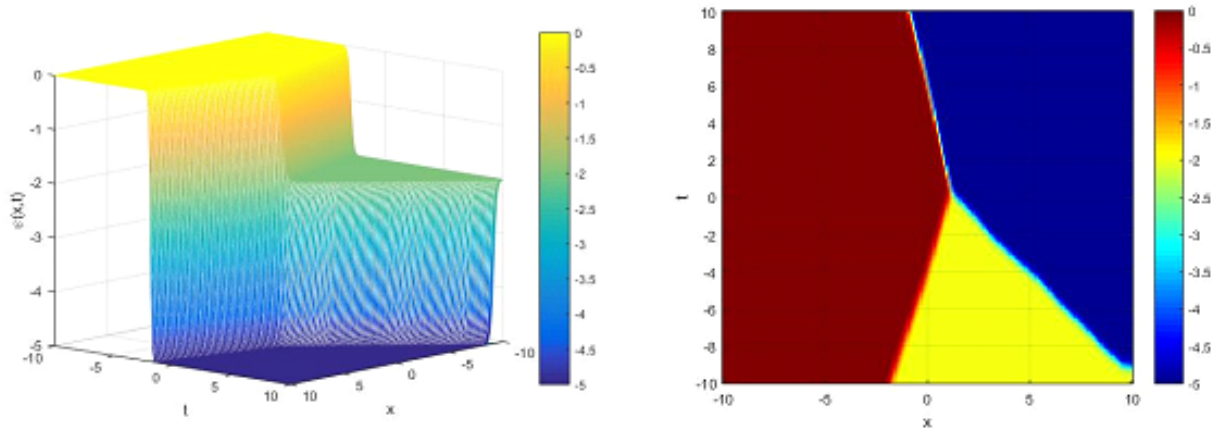

Fig. 11: illustrates the evolution of the anti-two–kink-shaped soliton solution described by Equation (31). Subfigure (a) provides a three-dimensional representation, while subfigure (b) shows the corresponding density plot. Both visualizations were generated using the parameter values$\sigma = 0$, $k_1 = -3$, $k_2 = 4$ $r_1 = -2$and $r_2 = -5$. These plots clearly depict the characteristic spatial configuration and propagation dynamics of the two–kink-shaped soliton.

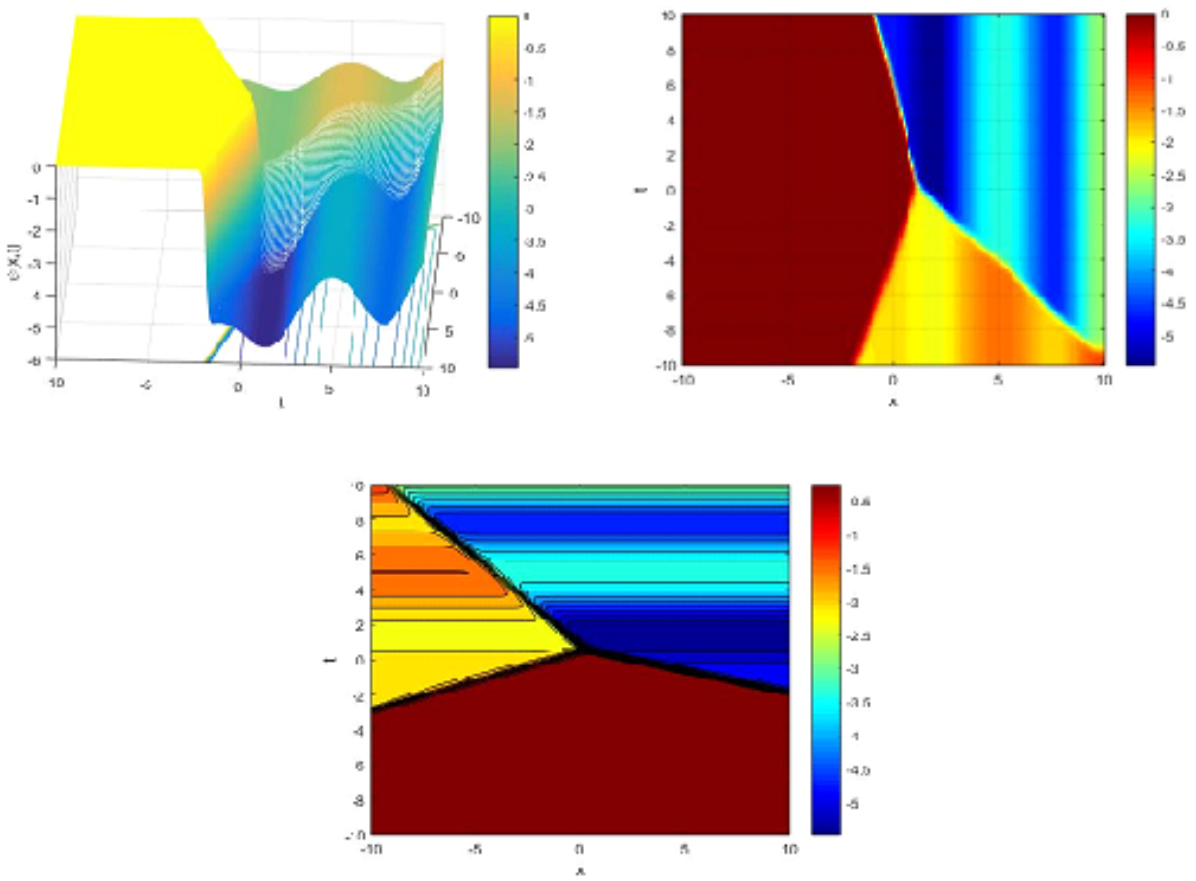

Fig. 12: presents the non-flat anti–two–kink-shaped soliton solution derived from Equation (31). (a) shows the three-dimensional surface plot, (b) depicts the corresponding density plot, (c) displays the heatmap. All visualizations were generated using the parameter values$\sigma = 0.3$, $k_1 = -3$, $k_2 = 4$ $r_1 = -2$and $r_2 = -5$. These results illustrate the impact of a small, nonzero noise parameter (σ) on the structure and temporal evolution of the anti–two–kink-shaped soliton.

rather than dispersive oscillations. The corresponding N-kink family generalizes this picture to multiple simultaneous fronts, providing an exact analytical representation of interacting discontinuity-like structures in (2+1) dimensions. Physically, such solutions model the concurrent presence of several sharp interfaces or wave fronts and their mutual interactions, including front collision and reconfiguration, which are characteristic of complex transport processes in fluids, plasmas, and other nonlinear media. When multiplicative white noise is introduced, the physical meaning of the solutions extends to the description of coherent fronts evolving under state-dependent random perturbations. Because the stochastic forcing scales with the local solution amplitude, fluctuations are most pronounced in dynamically active regions (particularly near steep gradients) so the noise effectively ”roughens” the front and induces random phase and amplitude modulation. For sufficiently small noise intensity, the kink structure remains recognizable and propagates with only mild stochastic wandering, indicating that the deterministic balance continues to dominate the dynamics. As the noise strength increases, however, the injected randomness competes more strongly with higher-order regularization and viscous dissipation, leading to visible deformation of the kink profile and, in extreme cases, partial loss of coherence and destabilization. In this way, the stochastic higher-order Burgers solutions provide a mathematically controlled mechanism for quantifying how random disturbances can either preserve, distort, or destroy shock-like nonlinear structures, thereby clarifying the dual role of noise as both a modulator of wave dynamics and a potential trigger for qualitative transitions in multidimensional nonlinear systems.

7 Conclusion and Future Work

In this study, a detailed theoretical and numerical investigation of the stochastic higher-order

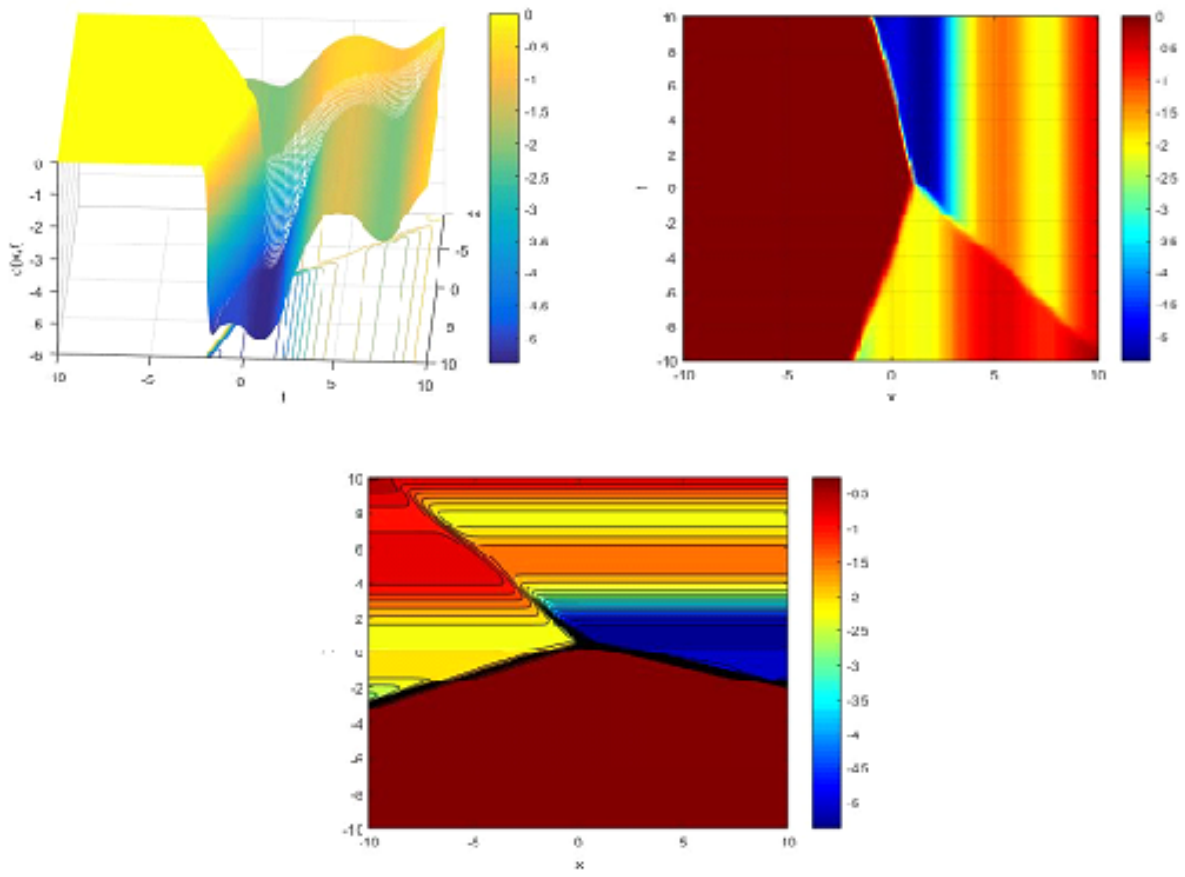

Fig. 13: presents the non-flat anti–two–kink-shaped soliton solution derived from Equation (31). (a) shows the three-dimensional surface representation, (b) illustrates the corresponding density plot, (c) depicts the heatmap. All visualizations were generated using the parameter values$\sigma = 0.6$, $k_1 = -3$, $k_2 = 4$ $r_1 = -2$and $r_2 = -5$. The results highlight the increased structural deformation of the anti–two–kink soliton as the noise intensity (σ) increases.

(2+1)-dimensional Burgers equation was conducted, with a particular focus on the behavior and stability of multi-kink soliton solutions under the influence of multiplicative noise. The analytical framework integrated the singular manifold method and a generalized Cole–Hopf transformation to derive explicit N-kink wave solutions, while the numerical simulations provided insight into the dynamic response of these structures under stochastic perturbations. Results confirm that the model admits rich and diverse soliton dynamics, capturing the essential features of nonlinear wave interactions, shock formation, and dissipative evolution in noisy environments. The simulation results highlighted the dual role of noise in nonlinear systems. While low-intensity stochastic fluctuations introduced minor deformations without compromising soliton coherence, higher noise levels significantly altered soliton morphology and led to a gradual destabilization of wave structures. These findings underscore the delicate balance between dispersion, nonlinearity, and stochasticity necessary to maintain soliton stability. Moreover, the study demonstrated the importance of parameter tuning (including wave numbers, propagation speeds, and noise coefficients) in enhancing solution robustness. The analytical and numerical methodologies presented here not only provide benchmarks for future modeling efforts but also lay the groundwork for noise-resilient design in practical applications such as spintronics, optical waveguides, and stochastic signal processing. Looking ahead, several directions merit further exploration. First, the inclusion of colored or spatially correlated noise, as opposed to idealized white noise, could yield more physically realistic insights into soliton behavior in natural systems. Second, extending the current analysis to fractional-order versions of the Burgers equation may offer deeper understanding of anomalous diffusion and memory effects. Third, experimental validation or data-driven calibration of model parameters would

strengthen the connection between theory and real-world systems. Finally, the development of adaptive numerical schemes tailored for higher-order stochastic PDEs would further improve the accuracy and efficiency of simulations in high-noise regimes. Collectively, these efforts can advance the theoretical foundation and practical applicability of stochastic nonlinear wave models across interdisciplinary domains.

References

[1] R. L. Mace and M. A. Hellberg, *Phys. Plasmas* **8**, 2649–2656 (2001).
[2] M. H. Islam, K. Khan, M. A. Akbar, and M. A. Salam, *SpringerPlus* **3**, 105 (2014).
[3] H. Naher, F. A. Abdullah, and M. A. Akbar, *PLoS One* **8**, e64618 (2013).
[4] H. Naher, F. A. Abdullah, and M. A. Akbar, *J. Appl. Math.* **2012**, 575387 (2012).
[5] S. A. El-Tantawy and W. M. Moslem, *Phys. Plasmas* **21**, 052112 (2014).
[6] D. Baldwin and W. Hereman, *Int. J. Comput. Math.* **87**, 1094–1119 (2010).
[7] A. S. Fokas, *Stud. Appl. Math.* **77**, 253–299 (1987).
[8] E. A.-B. Abdel-Salam, *Z. Naturforsch. A* **63**, 671–678 (2008).
[9] S. T. Rizvi *et al.*, *Results Phys.* **29**, 104654 (2021).
[10] E. A.-B. Abdel-Salam *et al.*, *Alexandria Eng. J.* **61**, 511–521 (2022).
[11] A.-M. Wazwaz, *Appl. Math. Comput.* **190**, 1198–1206 (2007).
[12] M. Zayed, G. Hassan, and E. A.-B. Abdel-Salam, *Math. Methods Appl. Sci.* **47**, 8366–8384 (2024).
[13] G. F. Hassan, E. A.-B. Abdel-Salam, and R. A. Rashwan, *Math. Methods Appl. Sci.* **46**, 2636–2650 (2023).
[14] A.-M. Wazwaz, *Appl. Math. Lett.* **25**, 1495–1499 (2012).
[15] Y. Z. Peng and E. Yomba, *Appl. Math. Comput.* **183**, 61–67 (2006).
[16] A. A. Hassaballa *et al.*, *Math. Comput. Model. Dyn. Syst.* **31**, 2595101 (2025).
[17] Z. M. H. El-Qahtani *et al.*, *Alexandria Eng. J.* **134**, 358–374 (2026).
[18] K. A. Alsatami, *AIMS Math.* **10**, 29189–29235 (2025).
[19] M. Ekici and C. A. Sarmasik, *Nonlinear Dyn.* **112**, 9459–9476 (2024).
[20] M. S. Ahmed, A. H. Arnous, and Y. Yildirim, *Ukrain. J. Phys. Opt.* **25**, 1111–1130 (2024).
[21] A. H. Arnous *et al.*, *Eur. Phys. J. Plus* **139**, 650 (2024).
[22] P. Imkeller and A. H. Monahan, *Stoch. Dyn.* **2**, 311–326 (2002).
[23] S. V. Lototsky and B. L. Rozovsky, *Stochastic Partial Differential Equations* (Springer, Berlin, 2017).
[24] B. Øksendal, *Stochastic Differential Equations* (Springer, Berlin, 2013).
[25] K. Sobczyk, *Stochastic Differential Equations* (Springer, Berlin, 2013).
[26] G. Cannizzaro and K. Chouk, *Ann. Probab.* **46**, 1710–1763 (2018).
[27] F. Flandoli, F. Russo, and J. Wolf, *Random Oper. Stoch. Equ.* **12**, 145–184 (2004).
[28] K. A. Alsatami, *Sci. Rep.* **15**, 19157 (2025).
[29] C. L. Wu and Y. X. Guo, *Acta Phys. Sin.* **59**, 5293–5298 (2010).
[30] A. A. Hassaballa *et al.*, *Mathematics Open* **4**, 2550013 (2025).
[31] H. M. Adel-Salam *et al.*, *Appl. Math. Inf. Sci.* **19**, 1369–1382 (2025).
[32] M. Zayed *et al.*, *AIMS Math.* **10**, 25907–25938 (2025).
[33] C. L. Wu, Y. X., *Acta Phys. Sin.* **59,** 5293–5298 (2010).
[34] Z. Yang, S. H. Ma, J. P. Fang, Chin. Phys. B **20**, 040301 (2011).

Faisal Muteb K. Almalki PhD-qualified academic mathematician. Specialized in applied mathematics, applied analysis, fluid mechanics, and numerical methods, with strong expertise in the formulation, analysis, and interpretation of mathematical models arising from physical and engineering systems. Demonstrates rigorous analytical reasoning, advanced problem-solving capability, and effective integration of computational tools with theoretical frameworks to address complex scientific problems.